Proceedings World Geothermal Congress 2020+1
Reykjavik, Iceland, April - October 2021

Linking Regional-Scale Crustal Structures to Small-Scale Geothermal Systems with Magnetotelluric Exploration: An Example from the Southeastern Canadian Cordillera

Cedar Hanneson, Martyn J. Unsworth and Theron Finley

Department of Physics, University of Alberta, Edmonton, Alberta, Canada, T6G 2E9

cedar@ualberta.ca

Keywords: Geothermal Exploration, Magnetotellurics, Electrical Resistivity, Rocky Mountain Trench, British Columbia, Canada

ABSTRACT

Understanding regional controls on the location and viability of geothermal resources is a key part of the geothermal exploration process and can increase the success-rate and cost-effectiveness of subsequent targeted reservoir-scale studies. The magnetotelluric (MT) method has been widely used in this exploration task as it can determine fluid distribution within the crust on both regional and local scales.

In the region 48-54°N and 112-122°W, we have assembled data from more than 300 broadband and long-period MT stations, including data from the LITHOPROBE transects, our own deployments, and those of other research groups. In this paper we apply this extensive MT dataset to geothermal exploration in the Southern Rocky Mountain Trench (SRMT), a major fault-controlled valley in southeastern British Columbia. The SRMT is a promising geothermal target as it is characterized by relatively high heat flow (~75 mW/m^2) and a number of surface geothermal features such as the Radium and Fairmont hot springs. It is thought that geothermal fluid circulation in the SRMT is controlled by fault structures, although the depth of the underlying heat source is uncertain. MT data can potentially detect the presence of fluids in fault zones in the upper crust, as well as the deeper sources of heat.

The MT data were converted into a resistivity model using a 3-D inversion algorithm, and the upper 80 km is presented and discussed in terms of the potential for future geothermal exploration. In our preliminary model, low resistivity zones are observed in the crust of southeastern British Columbia and likely indicate the presence of saline fluids, and perhaps partial melt in the lowermost crust. Crustal conductors beneath the SRMT are commonly, but not always, associated with hot springs, and may be representative of fluids in faults and reservoirs. An especially notable conductive feature occurs under the Canoe River hot spring and we have named it the Valemount Conductor. This feature is 10-20 km thick, extends horizontally for more than 100 km, and may represent a combination of saline fluids, partial melt, and conductive minerals. Future geophysical investigations, such as higher density MT deployments, are recommended for two regions in order to define the fine-scale crustal resistivity structure associated with these regional features: (1) the Redwall and Lussier River faults and (2) the SRMT northwest of Golden, BC.

1. INTRODUCTION

During the 1980's and 1990's, as part of the national LITHOPROBE project, extensive magnetotelluric (MT) data acquisition was undertaken in the Canadian Cordillera to study the distribution of fluids in the crust. However, the MT data collection was limited to profiles and 2-D inversion of the data could not constrain the crustal resistivity structure in 3-D. Since 2002, our research group at the University of Alberta has been systematically extending MT data coverage in the Canadian Cordillera to develop a fully 3-D regional-scale electrical resistivity model.

The study presented in this paper is centered on the Southern Rocky Mountain Trench (SRMT), a major fault-controlled valley in southeastern British Columbia. The region surrounding the SRMT is characterized by relatively high heat flow (~75 mW/m^2) and surface geothermal features such as the Radium and Fairmont hot springs occur along the valley floor, making it a promising geothermal target.

In this area, MT data have been collected at more than 300 locations by the LITHOPROBE project, University of Alberta, and other groups. Data in the region 48-54°N and 112-122°W were converted into a resistivity model using a 3-D inversion algorithm. The resistivity model extends to depths in excess of 300 km, but this paper only presents the uppermost 80 km and focuses on crustal features. Attention is drawn to features near the SRMT and the potential for future geothermal exploration is discussed. Further analyses and interpretations, and those concerned with the remainder of the model, will be presented in future publications.

2. BACKGROUND

2.1 Magnetotelluric Theory

The MT method uses natural electromagnetic (EM) signals to image the electrical resistivity of the subsurface and is widely used in geothermal exploration (Muñoz, 2014). The low-frequency radio wave sources are generated by global lightning activity and interactions between the solar wind and the Earth's ionosphere. This EM method measures time series of the electric and magnetic fields at the surface of the Earth, then converts them into frequency-domain transfer functions that describe the impedance of the

Earth. These transfer functions are used to calculate the electrical resistivity at depth. The theoretical foundations of the MT method were developed by Cagniard (1953) and a detailed description is given by Chave & Jones (2012).

The MT method has two main advantages that make it suitable for geothermal exploration:

1) It can effectively image aqueous and magmatic fluids, both of which are relevant to geothermal exploration. The electrical resistivity of the crust varies over several orders of magnitude: dry crystalline rock has a resistivity in excess of 1000 Ωm, whereas the presence of aqueous fluids or partial melt can lower this to values in the range 1-10 Ωm. Thus, fluid-rich zones are readily distinguished in MT data.

2) It can resolve crustal features over a broad range of depths allowing for investigation of both fine-scale crustal structure and deeper resistivity anomalies. The frequency of the passive radio wave source controls the depth of exploration according to the skin depth (δ) which is defined in metres as: $\delta \cong 500\sqrt{\rho T}$, where ρ is the bulk resistivity and T is the period of the signal. Therefore, longer periods give information about deeper structures and signals are more attenuated in lower resistivity materials. This broad depth range is a distinct advantage over other EM methods that are more limited in scale.

Resistivity models derived from MT data are an excellent way to detect fluids, although other causes of low resistivity such as hydrothermal alteration minerals (Ussher et al., 2000; Hersir et al., 2015), graphite films (Frost et al., 1989) and sulphide minerals (Varentsov et al., 2013) must also be considered. Additional geophysical and geological data are helpful in distinguishing between different low-resistivity materials.

The techniques available for the analysis of MT data have drastically improved over the past decade due to increased computing power. In the past, 1-D and 2-D inversions were used to derive models of sub-surface resistivity from MT data, but this greatly limited the application of the method in complex geological environments. MT data can now be inverted to produce 3-D resistivity models with new inversion codes that are run on multi-processor clusters (e.g., Kelbert et al., 2014; Lindsey and Newman, 2015).

2.2 Tectonic Setting

2.2.1 Geothermal Conditions

This study is focused on southeastern British Columbia (BC), with data coverage mainly in the Omineca, Foreland, and Intermontane belts of the Canadian Cordillera. In this region, heat flow is anomalously high, 70-120 mW/m^2 compared with the national average of 64±16 mW/m^2 (Majorowicz and Grasby, 2010). For comparison, an average of 85-90 mW/m^2 is observed in the Basin and Range, which hosts many of the United States' high-temperature (>150°C) geothermal systems (Wisian and Blackwell, 2004). The presence of more than forty thermal springs within our study area (Figure 1) is suggestive of the region's geothermal potential. It has previously been suggested that the locations of these thermal springs are controlled by faults (Grasby and Hutcheon, 2001) that allow deep circulation and consequent heating of meteoric water. Thermal springs in the study area include the Wolfenden, Radium, Fairmont, Red Rock, Lussier, Ram Creek, and Wildhorse hot springs near the SRMT (Grasby and Hutcheon, 2001; Allen et al., 2006). Aqueous geothermometry has indicated that the spring water reaches temperatures of ~40-100°C, implying circulation depths of ~2-5 km (Grasby and Hutcheon, 2001). While these temperatures are on the lower limit of what can be used to efficiently produce electricity, there is interest in using these systems for direct-use geothermal heating (Tuya Terra Geo Corp., 2016).

2.2.2 Bedrock Geology and Tectonics

The Canadian Cordillera is an ~800 km wide and ~2500 km long orogenic belt that covers much of British Columbia (BC) and Yukon, as well as the western edges of Alberta and the Northwest Territories. The Cordillera is widely regarded as an accretionary orogen, made up of several distinct terranes that were added to the North American margin throughout the Mesozoic and early Cenozoic. For simplicity, the Cordillera is often divided into five morphogeological belts based on bedrock type and geomorphology. From west to east, they are: (1) the Insular belt, (2) the Coast belt, (3) the Intermontane belt, (4) the Omineca belt, and (5) the Foreland belt. This study is primarily focused on geothermal systems in the Omineca and Foreland belts, but a brief summary of all five belts is provided below due to their intertwined tectonic history.

The Insular belt is a region of moderate topography that encompasses Vancouver Island, Haida Gwaii, and the westernmost mainland of BC. Its bedrock is largely igneous, including extensive basalt flows and granitic intrusions. The Coast belt encompasses the high-elevation, extensively glaciated mountain range that runs the length of western BC and is dominantly made up of large plutonic complexes associated with the subduction that led to the Cretaceous to Eocene accretion of the Insular belt terranes. Modern continental arc volcanoes associated with the Cascadia subduction zone have developed on top of the Mesozoic plutonic complex. The Intermontane belt is an elevated plateau with subdued relief and is dominantly made up of island arc volcanic rocks and associated sedimentary sequences. The Omineca belt is a mountainous region dominantly composed of mid to high-grade meta-sedimentary rocks, as well as numerous continental arc-type plutonic suites. The Foreland belt encompasses the rugged Canadian Rocky Mountains, which are composed of the largely unmetamorphosed but highly deformed sedimentary rocks that once formed the ancient North American passive margin.

Accretion of the various exotic island-arc terranes of the Intermontane and Insular belts resulted in contractional deformation from the Jurassic to the Eocene, giving rise to the Cordillera. Following the cessation of orogenesis, the southern Cordillera underwent widespread crustal extension in the Eocene, which was accommodated on an array of normal faults, many of which run through our study area in southeast BC (Parrish et al., 1988). Some of these Eocene-aged normal faults have been reactivated as dextral strike-slip faults in response to far-field stress from the active Cascadia subduction zone (Finley, 2020). The present-day deformation is especially relevant for understanding geothermal systems for two reasons: (1) extension provides a mechanism for crustal thinning

and an increased geothermal gradient, and (2) recently active faults are more likely to be permeable conduits allowing convection of thermal water from depth to the surface.

2.2.3 Shallow and Deep Lithospheric Structure

This study is focused on the Southern Rocky Mountain Trench (SRMT), and the faults that occur within and adjacent to it. These faults include: the SRMT fault, Purcell Thrust fault, Redwall fault, and Lussier fault. The SRMT fault occupies the SRMT for much of its length, though there are limited outcrop exposures of the fault itself. The fault dips steeply west and estimates of normal dip-slip displacement range from 2-10 km (van der Velden and Cook, 1996; McDonough and Simony, 1988; Gal and Ghent, 1990). The across-fault continuity of several transverse features, both structural and stratigraphic, indicate that it does not exhibit significant strike-slip offset (McMechan and Thompson, 1989), though Finley (2020) suggested the possibility of post-Eocene dextral offset on the order of tens of kilometers. The Purcell Thrust fault is located within the SRMT from 51.5°N (north of Golden) to 50.5°N (near Invermere). This fault is regarded as an out-of-sequence thrust fault that developed during the last stages of Mesozoic compression. Notably, no thermal springs occur along SRMT where the Purcell Thrust occurs, suggesting this structure may not be conducive to fluid circulation. The Redwall and Lussier faults run parallel with and to the east of the SRMT, between the towns of Radium and Cranbrook. These faults are not well-studied, and have variably been interpreted as dextral, sinistral, or thrust faults (North and Henderson, 1954; Charlesworth, 1959; Foo, 1979). Many thermal springs along the southern SRMT in fact coincide with these faults rather than the main SRMT fault, hence their inclusion in this study.

The deeper lithospheric structure in the study area has previously been investigated using a variety of geophysical techniques, e.g., 2-D inversion of MT data (Rippe et al., 2013), multimode seismic waveform inversion (Schaeffer and Lebedev, 2014), Rayleigh wave tomography (Bao and Eaton, 2015), and finite-frequency seismic tomography (Chen et al., 2018). Hyndman and Lewis (1999) summarized that the Moho is at 32-34 km depth in the Canadian Cordillera and 40-50 km depth in the adjacent craton. Bennett et al. (1975) modelled the Moho at 51-58 km depth near the SRMT. The Moho marks a sharp increase in seismic wave velocity with depth, but the contrast in composition and density do not lead to a coincident change in electric properties. Hence, electromagnetic methods are inherently insensitive to the Moho; however, if fluids are bounded by this interface, its location may be inferred. Deep crustal aqueous fluids tend to occur in the 400-700°C temperature range (Hyndman and Shearer, 1989) and in the southern Canadian Cordillera, Moho temperatures are approximately 800-1000°C (Currie and Hyndman, 2006); therefore, deep water is most likely to occur in the crust in the 10-30 km depth range. However, fluids in geothermal systems in the southern Canadian Cordillera have been interpreted to be meteoric in origin, circulating to depths less than 5 km (Grasby and Hutcheon, 2001). Water in the lower crust may be derived from dehydration of oceanic crust and sediments in subduction zones, and devolatilization of upwelling mantle (Hyndman and Shearer, 1989, and references therein).

The Cordilleran lithosphere is relatively thin, which is due, in part, to crustal extension and thinning in the Eocene. The lithosphere-asthenosphere boundary (LAB) in this region is at a depth of 50-60 km (Monger and Price, 2002; Hyndman et al., 2005). Based on observed thermal conditions, such as high surface heat flow (~75 mW/m^2), vigorous convection in the asthenosphere is believed to occur (Currie et al., 2004; Hyndman et al., 2005). In southwestern Alberta, the depth of the LAB increases to greater than 180 km (Bao and Eaton, 2015), which is at least three times the value observed in the southern Cordillera. This thick lithosphere is part of the North American craton.

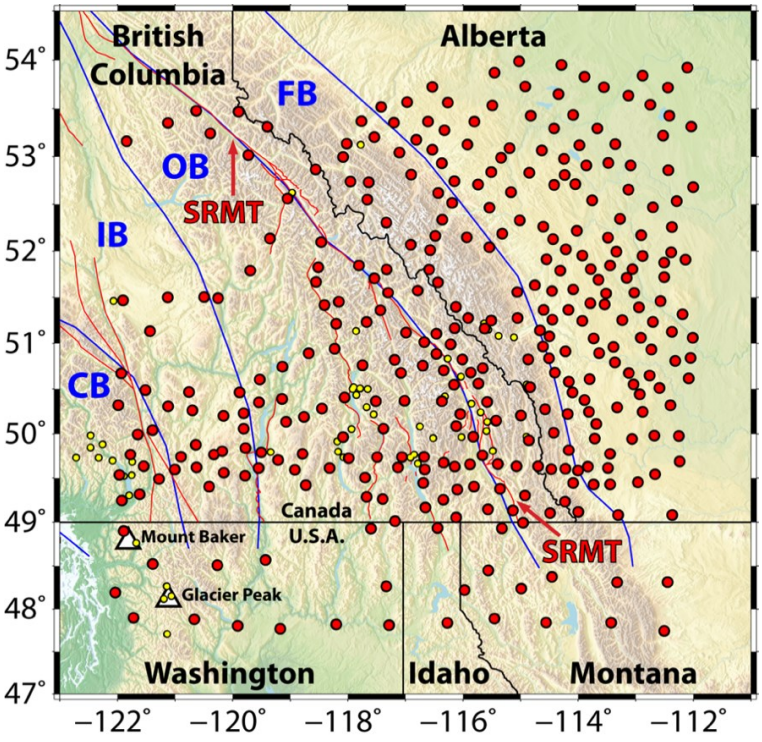

Figure 1: MT stations (red dots) used in the geophysical inversion to create the electrical resistivity model. The approximate north-south extent of the SRMT topographic lineament is indicated by the red arrows. Political boundaries (black lines), morphogeological boundaries (blue lines), major faults (red lines), and thermal springs (yellow dots) are also shown. CB = Coast Belt, IB = Intermontane Belt, OB = Omineca Belt, FB = Foreland Belt.

3. DATA AND METHODS

This study used data from 336 MT sites in the region 47.7 to 54°N, and 112 to 122°W (Figure 1). These data included 110 Lithoprobe sites, 22 EarthScope USArray sites, and 19 sites from other previous studies. Our research group collected an additional 185 MT soundings between 2002 and 2018. This large grid enhances the model precision in southeastern British Columbia, our area of interest, by extending the data coverage beyond the southern Omineca belt on all four sides, compared with restricting data to a smaller area. In previous decades, inversion of MT data was limited to 1-D and 2-D, producing resistivity models that were limited in their ability to adequately represent Earth structure. 3-D inversion has become practical in recent years through the development of new inversion algorithms that run on multi-processor clusters. The MT transfer functions (impedance and tipper) were jointly inverted using the ModEM algorithm (Kelbert et al., 2014). The inversion used data at 18 periods, logarithmically spaced between 1 and 18,000 s, and Figure 2 shows how many stations had data at each of these periods. Tipper data were omitted at the two longest periods; when they were included, they resulted in the highest misfit of any single-component single-period misfit. Furthermore, Meqbel et al. (2014) omitted tipper data at periods longer than 6500 s to avoid external source bias, in alignment with our methods.

The 336 sites were chosen for data quality and to ensure that station spacing was as uniform as possible, given the available MT data (more than 700 sites in total). The median distance between a station and its nearest neighbour was 22 km. The data were measured in geomagnetic coordinates: magnetic north and east for x and y, respectively. For the inversion they were rotated to a geographic coordinate system: geographic north and east for x and y, respectively. The following error floors were applied to the impedance ($\boldsymbol{Z}$) and tipper ($\boldsymbol{T}$) data: 5% of $\sqrt{(|Z_{xy}||Z_{yx}|)}$ to Z_{xy} and Z_{yx}, 10% of $\sqrt{(|Z_{xy}||Z_{yx}|)}$ to Z_{xx} and Z_{yy}, and 0.03 to T_{zx} and T_{zy}, where $\boldsymbol{Z}$ is a complex-valued 2x2 tensor and $\boldsymbol{T}$ is a complex-valued 2x1 vector. These are the same error floors used by Wang (2019).

The study area is approximately 700 km x 700 km; therefore, a relatively coarse mesh was used. The model cells were 5 km x 5 km in the horizontal plane, with 12 padding cells increasing geometrically by a factor of 1.4 away from the central grid. Given the extent of the study area, this was the finest grid allowed by a reasonable amount of memory on a parallel computing cluster; the inversion required roughly 500 GB of memory for nearly four weeks. During data selection, locations were chosen to ensure that a minimum of two vacant grid cells separated any two MT sites. The uppermost layer was 50 m thick, and the layer thickness increased geometrically by a factor of 1.15 downward. The total model volume was 2,689 km in the north-south direction, 2,709 km in the east-west direction, and 1,105 km in the vertical direction, allowing a significant buffer around the study area. At the longest period in our dataset, the skin depth in a 100 Ωm half-space is 679 km; therefore, the model extended approximately 1.5 skin depths in all directions. Due to the coarseness of the mesh and the computing resources needed, topography and bathymetry were not included in the model. The rectangular model mesh used in this study had 1.76 million cells: 172 in the north-south direction, 176 in the east-west direction, and 58 in the vertical direction.

The model covariance was 0.3 in the horizontal directions and 0.4 in the vertical direction, thereby allowing for lateral resistivity variations that were less smooth than variations with depth. The model had a tear halfway through the sedimentary basins of the upper crust, as determined by the CRUST 1.0 model (Laske et al., 2013), meaning that the model covariance was reduced to zero at these interfaces and no smoothing was imposed across the tear. It allowed for sharp resistivity transitions as might be expected from the layered sedimentary geology of the Western Canada Sedimentary Basin. Typical sedimentary strata in this region are Cretaceous siliciclastic rocks overlying Devonian carbonate rocks and since the latter are more resistive, it is reasonable to place a tear within the sedimentary layer. This initial condition had little effect on the resistivity structure beneath the Cordillera, but it was used because it did affect the resistivity structure beneath the WCSB (not presented here but will be discussed in future publications involving this model). The inversion started with a regularization parameter (λ) of 1 and this value decreased, one order of magnitude at a time, to a minimum value of 10^{-8} by the end of the inversion. This created smooth models at early iterations, then allowed more complex structures to emerge as the inversion progressed.

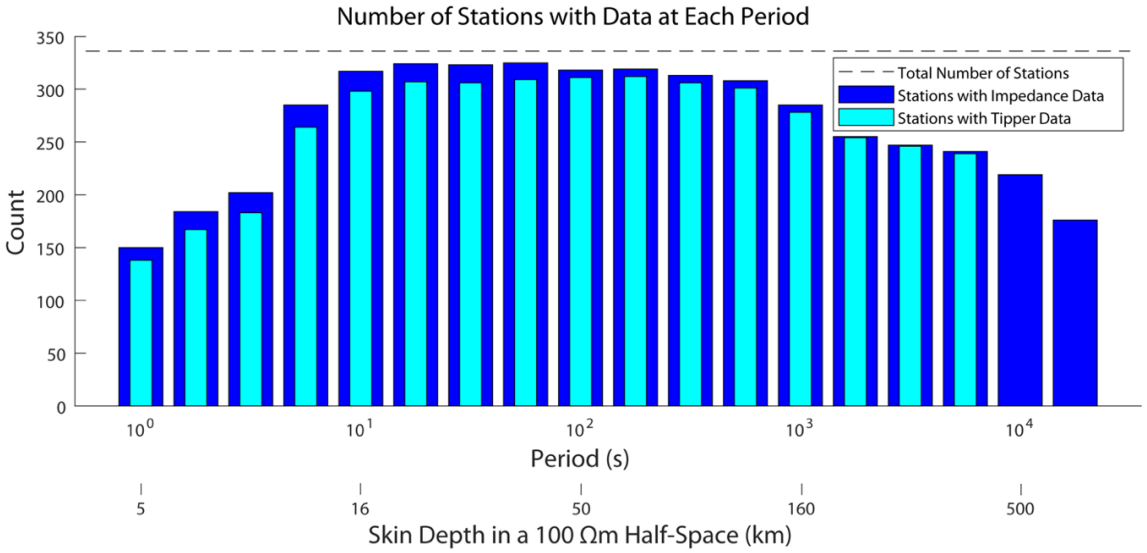

Figure 2: MT data periods and the number of stations with data at each period. Tipper data were omitted at the two longest periods. Sample skin depth calculations are included for reference.

4. RESISTIVITY MODEL

A number of 3-D inversions were run to examine the dependence on the control parameters. The preferred inversion used a starting model with 10 Ωm above the tear in the sedimentary rocks and 100 Ωm everywhere else. After 297 iterations, the inversion converged to an r.m.s. misfit of 2.23 from a starting value of 16. Several stations near the SRMT had particularly large misfits which could be the result of electrical anisotropy in the crust. The ModEM algorithm (Kelbert et al., 2014) assumes electrically isotropic structure and 3-D anisotropic codes are still in the development stage (e.g., Kong et al., 2020, in revision). Regions without MT data coverage remained at 100 Ωm in the model and are unconstrained, e.g., some northwestern parts of the study area (Figure 1).

A map of misfit by station is shown in Figure 3. Many of the sites with high misfit were located in the eastern Omineca belt and western Foreland belt, a region of suspected anisotropy, and further investigation is required. For example, Lee (2020) performed isotropic and anisotropic 3-D inversions near the SRMT fault at Kinbasket Lake, and preferred the anisotropic model over the isotropic model, based on geological considerations. Detailed interpretation of this preliminary model may change, but the general observations are likely robust. With the exception of a few outliers, sites westward of and in the western Omineca belt had low misfit. Sites in the WCSB generally had low misfit, with the exceptions often caused by data at the shortest and longest periods. The six different data components had very similar misfit, hence the joint inversion successfully fit the impedance and tipper data similarly well.

Our model shows broad similarities with previous MT studies in the Canadian Cordillera. Rippe et al. (2013) used 2-D inversion of MT data to create a pair of sub-parallel resistivity models of the southern Canadian Cordillera and they imaged a crustal conductor beneath the Intermontane and Omineca belts. On their southern profile, the top was at ~20 km depth, and a similar but weaker conductor was observed on their northern model. These lower crustal conductors were interpreted as saline fluids and/or partial melt, with the weaker northern conductor inferred to be due to the reduced extension. Our model shows a similar crustal conductor, but it is shallower and has a more complex 3-D structure than in the 2-D studies. Rippe et al. (2013) also showed that the low resistivity of the upper mantle was consistent with the presence of a shallow asthenosphere.

In the model, the Canadian Cordillera in southeastern BC is characterized by resistive upper crust and numerous discrete mid- and lower-crustal conductors. To the east beneath the plains of Alberta, the high-resistivity North American craton is overlain by the low-resistivity WCSB. Three horizontal slices of the preferred resistivity model are presented in Figure 4. A band of low resistivity west of the BC-Alberta border is observed at crustal depths of 5-30 km (e.g., Figure 4a-b). This lateral change in resistivity structure corresponds roughly to the well-documented facies boundary between the Paleozoic carbonate platform to the east and the shale-dominated oceanic basin to the west. Rocks in the shale basin are more commonly ductily-deformed, and show pervasive penetrative cleavage and low-grade metamorphism, whereas the eastern carbonate rocks are typically brittly-deformed, and unmetamorphosed. It has been suggested that the facies boundary is the trace of a continental suture (Johnston, 2008; Chen et al., 2019) which may explain the contrasting electrical properties we observe on either side. At depths greater than 25 km, there could be partial melting in the southern Omineca belt (Ledo and Jones, 2001) and several large conductors extend below this depth in our model. At shallower depths, low resistivity is more likely caused by interconnected saline fluids. Figure 4c shows the model layer at a depth of 51-58 km which is close to the Moho depth near the SRMT (Bennett et al., 1975).

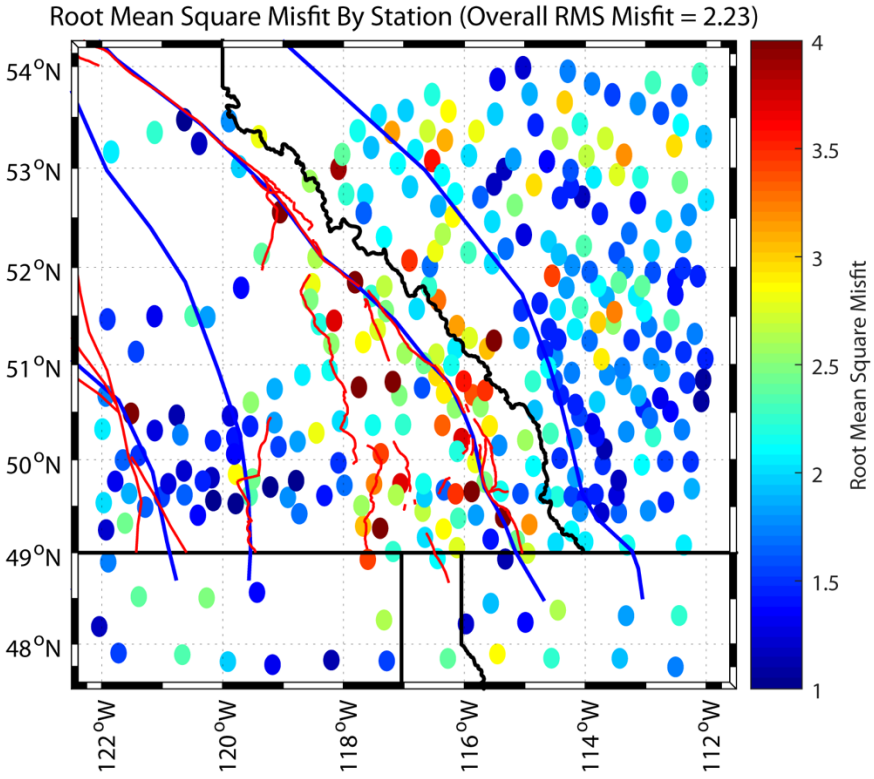

Figure 3: Root-Mean-Square (RMS) misfit at each of the MT sites. The overall RMS misfit is 2.23. Political boundaries (black lines), morphogeological boundaries (blue lines), and major faults (red lines) are also shown.

A vertical slice is presented in Figure 5. The profile A-B-C is roughly parallel with the SRMT and passes eight thermal springs. The northernmost of them, Canoe River hot spring, is associated with a large low-resistivity anomaly that we name the Valemount Conductor (VC). This oblong, NW-SE-trending crustal conductor is least resistive (< 1 Ωm) beneath the Canoe River hot spring and is 10-20 km thick for much of its length. To the northwest of the hot spring, it dips at ~45° to a depth of ~60 km, and to the southeast it extends horizontally for more than 100 km below Kinbasket Lake. The VC is the deepest of the various conductors resolved in our model beneath the SRMT. The depth to the base of a conductor is poorly resolved by the MT method, therefore it cannot be determined if the VC extends into the mantle. The VC is located in the footwall of the SRMT fault, a westward dipping normal fault. The low resistivity could be caused by saline fluids in porous fractured rocks near the fault and/or conductive minerals (e.g., graphite, sulphides, or clays) deposited by prior fluid flow. Lee (2020) interpreted a shallow crustal conductor near the SRMT fault in the same region as more likely caused by graphite or sulphides than aqueous fluids.

The seven hot springs near profile B-C occur along a series of faults: Wolfenden and Radium hot springs are near the southern end of the Purcell Thrust Fault and the northern end of the Redwall Fault; Fairmont and Red Rock hot springs are near the Redwall Fault; and Lussier Canyon, Ram Creek, and Wildhorse hot springs are near the Lussier River Fault. There are a few mid-crustal conductors beneath this cluster of hot springs, predominantly in the 11-33 km depth range (Figure 5). The observed low resistivity is likely caused by aqueous fluids as these depths are within the 400-700°C temperature range (Hyndman and Shearer, 1989; Currie and Hyndman, 2006). The pattern of sub-parallel, discrete conductors in the middle of profile A-B-C could be caused by electrical anisotropy (e.g., Heise and Pous, 2001) and will be subject to further investigation, such as forward modelling and anisotropic 3-D inversion.

Very low resistivity is observed in the upper and middle crust, extending ~100 km to the NW from point B, but there is a conspicuous absence of hot springs in this region. This section of the profile is near the Cretaceous Purcell Thrust Fault, which was not reactivated by Eocene extension nor modern transpression and is therefore likely not permeable. This low-resistivity anomaly is shallowest beneath the Columbia River northwest of Golden, BC. The low resistivity could be caused by conductive minerals deposited by prior fluid flow associated with the extinct Purcell Thrust; however, we cannot exclude the possibility of saline fluids trapped beneath an impermeable layer or diffused within a permeable layer such that they do not form a discrete hot spring at the surface. This region is recommended for future geophysical research, for example, a higher frequency MT survey with shorter interstation distances. If possible, the resulting dataset should be inverted using a 3-D anisotropic inversion program (e.g., Kong et al., 2020, in revision). Conductors associated with other clusters of hot springs, in the central southern Omineca belt for example, will be presented and discussed in the future.

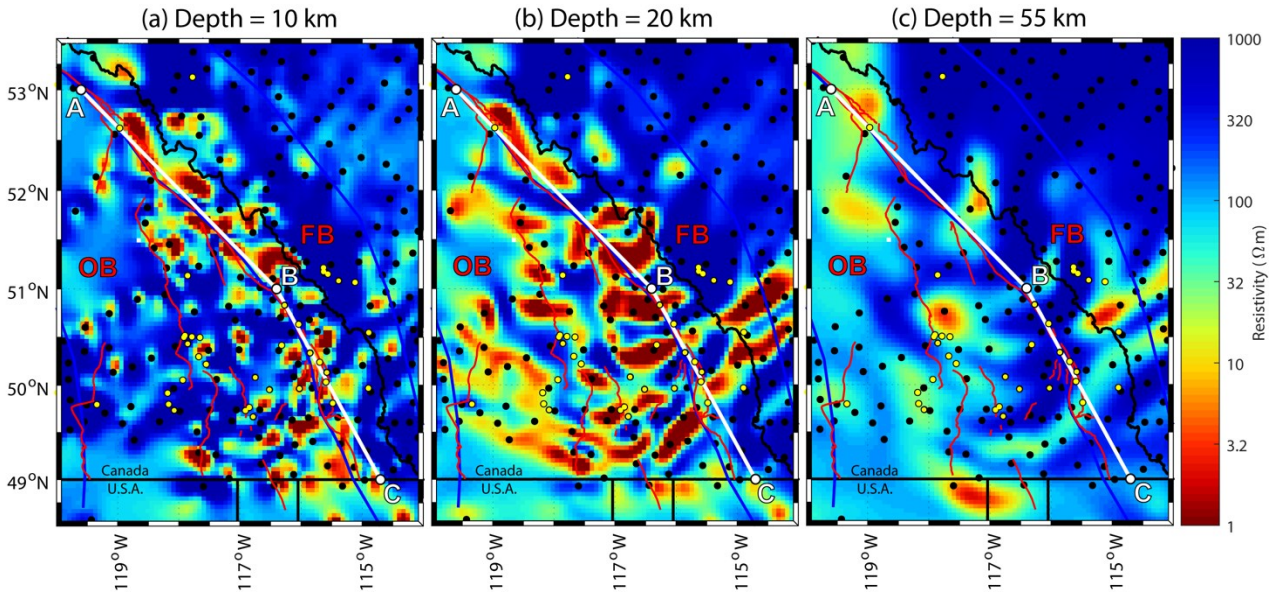

Figure 4: Horizontal slices of the resistivity model in the region 48.5-53.5°N and 114-120°W at depths of: (a) 9-11 km, (b) 19-22 km, and (c) 51-58 km. Political boundaries (black lines), morphogeological boundaries (blue lines), major faults (red lines), thermal springs (yellow dots), and MT sites (black dots) are also shown. OB = Omineca Belt and FB = Foreland Belt. A cross-section along profile A-B-C is shown in Figure 5.

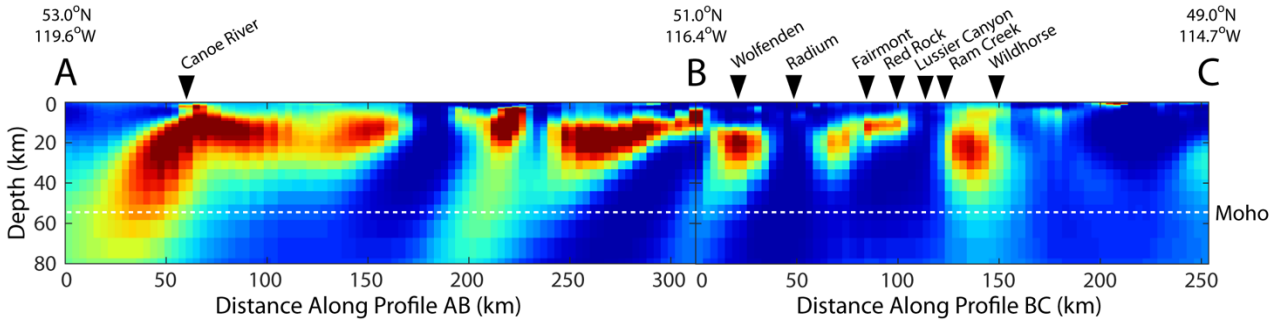

Figure 5: Vertical slices of the resistivity model in the vicinity of the Southern Rocky Mountain Trench, along with the locations of eight nearby thermal springs. The location of profile A-B-C and the resistivity colour scale are shown in Figure 4. Approximate Moho depth (white dashed line) is from a seismic refraction model (Bennett et al., 1975).

5. CONCLUSIONS

The 3-D inversion model presented here has similar regional resistivity structure to that imaged by the 2-D analysis of Rippe et al. (2013). This showed that the mid-crust of the southern Canadian Cordillera was characterized by low resistivity, which is most likely interpreted as a layer of aqueous fluids that may be underlain by partial melt.

Our new 3-D model shows that the mid-crustal layer is composed of a number of discrete low resistivity zones. Some of these appear to underlie regions with mapped geothermal manifestations, while others do not. It may be that some of these discrete zones are representative of "blind" geothermal systems that do not have surface manifestations. However, the observed pattern may also be indicative of strong crustal anisotropy that is poorly resolved with this isotropic inversion.

As these results are still preliminary, we plan to undertake research in two new directions: (1) application of a new 3-D anisotropic MT inversion algorithm to test the validity of the discrete conductors, and (2) densification of the MT grid in regions of interest to detect fluid pathways from the mid-crustal layer to the surface. A finer model mesh and higher frequency data would allow the resolution of smaller and shallower features. Two examples of possible target areas are: (1) a region encompassing the Redwall and Lussier River faults, where there are several known hot springs, and (2) the SRMT northwest of Golden, BC, where there is a notable absence of thermal springs. Modelling of the upper-crustal (e.g., top 5 km) resistivity structure, especially with the addition of topography, could image specific hydrothermal systems associated with known hot springs, and possibly locate potential blind geothermal systems.

REFERENCES

Allen, D. M., Grasby, S. E., and Voormeij, D. A.: Determining the circulation depth of thermal springs in the southern Rocky Mountain Trench, south-eastern British Columbia, Canada using geothermometry and borehole temperature logs, *Hydrogeology Journal*, **14**, (2006), 159-172.

Bao, X. and Eaton, D. W.: Large variations in lithospheric thickness of western Laurentia: Tectonic inheritance or collisional reworking? *Precambrian Research*, **266**, (2015), 579-586.

Bennett, G. T., Clowes, R. M., and Ellis, R. M.: A seismic refraction survey along the southern Rocky Mountain Trench, Canada, *Bulletin of the Seismological Society of America*, **65**, (1975), 37-54.

Cagniard, L.: Basic theory of the magneto-telluric method of geophysical prospecting, *Geophysics*, **18-3**, (1953), 605-635.

Charlesworth, H. A. K.: Some suggestions on the structural development of the Rocky Mountains of Canada, *Journal of the Alberta Society of Petroleum Geologists*, **7-11**, (1959), 249-256.

Chave, A. D. and Jones, A. G.: The magnetotelluric method: Theory and practice, *Cambridge University Press*, (2012).

Chen, Y., Gu, Y. J., and Hung, S.: A new appraisal of lithospheric structures of the cordillera-craton boundary region in western Canada, *Tectonics*, **37-9**, (2018), 3207-3228.

Chen, Y., Gu, Y. J., Currie, C. A., Johnston, S. T., Hung, S., Schaeffer, A. J., and Audet, P.: Seismic evidence for a mantle suture and implications for the origin of the Canadian Cordillera, *Nature Communications*, **10**, (2019), 1-10.

Currie, C. A. and Hyndman, R. D.: The thermal structure of subduction zone back arcs, *Journal of Geophysical Research*, **111**, (2006), 1-22.

Currie, C. A., Wang, K., Hyndman, R. D., and He, J.: The thermal effects of steady-state slab-driven mantle flow above a subducting plate: the Cascadia subduction zone and backarc, *Earth and Planetary Science Letters*, **223**, (2004), 35-48.

Finley, T.: Fault-hosted geothermal systems in southeastern British Columbia, *M.Sc. Thesis*, (2020), University of Alberta, Edmonton, Canada.

Foo, W. K.: Evolution of transverse structures linking the Purcell Anticlinorium to the western Rocky Mountains near Canal Flats, British Columbia, *Ph.D. Thesis*, (1979), Queens University, Kingston, Canada.

Frost, B. R., Fyfe, W. S., Tazaki, K., and Chan, T.: Grain-boundary graphite in rocks and implications for high electrical conductivity in the lower crust, *Nature*, **340**, (1989), 134-134.

Gal, L. P. and Ghent, E. D.: Metamorphism in the Solitude Range, southwestern Rocky Mountains, British Columbia: comparison with adjacent Omineca Belt rocks and tectonometamorphic implications for the Purcell Thrust, *Canadian Journal of Earth Sciences*, **27-11**, (1990), 1511-1520.

Grasby, S. E. and Fergusson, G.: Controls on the distribution of thermal springs in the Canadian Cordillera, *Proceedings World Geothermal Congress*, (2010), 1-4.

Grasby, S. E. and Hutcheon, I.: Controls on the distribution of thermal springs in the southern Canadian Cordillera, *Canadian Journal of Earth Sciences*, **38**, (2001), 427-440.

Gupta, J. C. and Jones, A. G.: Electrical conductivity structure of the Purcell Anticlinorium in southeast British Columbia and northwest Montana, *Canadian Journal of Earth Sciences*, **32-10**, (1995), 1564-1583.

Heise, W. and Pous, J.: Effects of anisotropy on the two-dimensional inversion procedure, *Geophysical Journal International*, **147**, (2001), 610-621.

Hersir, G. P., Árnason, K., and Vilhjálmsson, A. M.: 3D inversion of magnetotelluric (MT) resistivity data from Krýsuvík high temperature geothermal area in SW Iceland, *Proceedings World Geothermal Congress*, (2015), 1-14.

Hyndman, R. D., Currie, C. A., and Mazzotti, S. P.: Subduction zone backarcs, mobile belts, and orogenic heat, *GSA Today*, **15-2**, (2005), 4-10.

Hyndman, R. D. and Shearer, P. M.: Water in the lower continental crust: modelling magnetotelluric and seismic reflection results, *Geophysical Journal International*, **98**, (1989), 343-365.

Johnston, S. T.: The Cordilleran Ribbon Continent of North America, *Annual Reviews of Earth and Planetary Sciences*, **36**, (2008), 495-530.

Kelbert, A., Meqbel, N., Egbert, G. D., and Tandon, K.: ModEM: A modular system for inversion of electromagnetic geophysical data, *Computers and Geosciences*, **66**, (2014), 40-53.

Kong, W., Tan, H., Lin, C., Unsworth, M. J., Lee, B. M., Peng, M., Wang, M., and Tong, T.: Three-dimensional inversion of magnetotelluric data for a resistivity model with arbitrary anisotropy, *Journal of Geophysical Research*, (2020), in revision.

Laske, G., Ma, Z., Masters, G., and Pasyanos, M.: CRUST 1.0: a new global crustal model at 1 x 1 degrees, (2013), downloaded from https://igppweb.ucsd.edu/~gabi/crust1.html

Ledo, J. and Jones, A. G.: Regional electrical resistivity structure of the southern Canadian Cordillera and its physical interpretation, *Journal of Geophysical Research*, **106-12**, (2001), 30755-30769.

Lee, B.: Improving exploration for geothermal resources with the magnetotelluric method, *Ph.D. Thesis*, (2020), University of Alberta, Edmonton, Canada.

Lindsey, N. J. and Newman, G. A.: Improved workflow for 3D inverse modeling of magnetotelluric data: Examples from five geothermal systems, *Geothermics*, **53**, (2015), 527-532.

Majorowicz, J. and Grasby, S. E.: Heat flow, depth-temperature variations and stored thermal energy for enhanced geothermal systems in Canada, *Journal of Geophysics and Engineering*, **7**, (2010), 232-241.

McDonough, M. R. and Simony, P. S.: Structural evolution of basement gneisses and Hadrynian cover, Bulldog Creek area, Rocky Mountains, British Columbia, *Canadian Journal of Earth Sciences*, **25**, (1988), 1687–1702.

McMechan, M. E. and Thompson, R. I.: Structural style and history of the Rocky Mountain fold and thrust belt, *Western Canada Sedimentary Basin: A Case History*, (1989), 47-71.

Meqbel, N. M., Egbert, G. D., Wannamaker, P. E., Kelbert, A., and Schultz, A.: Deep electrical resistivity structure of the northwestern U.S. derived from 3-D inversion of USArray magnetotelluric data, *Earth and Planetary Science Letters*, **402**, (2014), 290-304.

Monger, J. and Price, R.: The Canadian Cordillera: Geology and tectonic evolution, *CSEG Recorder*, **27-2**, (2002), 17-36.

Muñoz, G.: Exploring for Geothermal Resources with Electromagnetic Methods, *Surveys in Geophysics*, **35**, (2014), 101-122.

North, F. K. and Henderson, G. G. L.: The Rocky Mountain Trench, *Canadian Society of Petroleum Geologists*, Guide Book Fourth Annual Field Conference Banff-Golden-Radium, (1954), 82-100.

Parrish, R. R., Carr, S. D., and Parkinson, D. L.: Eocene extensional tectonics and geochronology of the Southern Omineca Belt, British Columbia and Washington, *Tectonics*, **7-2**, (1988), 181-212.

Rippe, D., Unsworth, M. J., and Currie, C. A.: Magnetotelluric constraints on the fluid content in the upper mantle beneath the southern Canadian Cordillera: Implications for rheology, *Journal of Geophysical Research*, **118**, (2013), 5601–5624.

Schaeffer, A. J. and Lebedev, S.: Imaging the North American continent using waveform inversion of global and USArray data, *Earth and Planetary Science Letters*, **402**, (2014), 26-41.

Tuya Terra Geo Corp.: Direct-use Geothermal Resources in British Columbia, *Summary of Findings*, Geoscience BC Report 2016-07, Contract 2015-22, (May 5, 2016), 1-38.

Ussher, G., Harvey, C., Johnstone, R., and Anderson, E.: Understanding the resistivities observed in geothermal systems, *Proceedings World Geothermal Congress*, (2000), 1915-1920.

van der Velden, A. J. and Cook, F. A.: Structure and tectonic development of the southern Rocky Mountain trench, *Tectonics*, **15**, (1996), 517–544.

Varentsov, I. M., Kulikov, V. A., Yakovlev, A. G., and Yakovlev, D. V.: Possibilities of magnetotelluric methods in geophysical exploration for ore minerals, *Physics of the Solid Earth*, **49-3**, (2013), 309-328.

Wang, E.: Multidimensional magnetotelluric studies of the Precambrian Alberta basement, *Ph.D. Thesis*, (2019), University of Alberta, Edmonton, Canada.

Wisian, K. W. and Blackwell, D. D.: Numerical modeling of Basin and Range geothermal systems, *Geothermics*, **33**, (2004), 713-741.